Native collagen VI delays muscle stem cell early differentiation

Samuele Metti‡, Francesco Da Ros*,‡, Giorgia Toniato, Matilde Cescon and Paolo Bonaldo§

Department of Molecular Medicine, University of Padova, 35131 Padova, Italy

*Present address: SOSd Cell Stem Unit, Department of Translational Research, CRO Aviano, National Cancer Institute, IRCSS, 33081 Aviano, Italy.
‡These authors contributed equally to this work
§Author for correspondence (bonaldo@bio.unipd.it)

Keywords: Extracellular matrix; Skeletal muscle; Muscle stem cells; Collagen VI.

Summary statement

Collagen VI, a pivotal extracellular regulator of muscle homeostasis, counteracts myogenic differentiation and sustains stemness by modulating intracellular signals involved in myogenesis.

Abstract

Adult muscle stem cells (MuSCs) are critical for muscle homeostasis and regeneration, and their behavior relies on a finely regulated niche made of specific extracellular matrix (ECM) components and soluble factors. Among ECM proteins, collagen VI (Col6) influences the mechanical properties of the niche and, in turn, MuSC self-renewal capabilities. Here we investigated whether Col6 can exert a direct function as a biochemical signal for regulating the stemness and differentiation processes of murine MuSCs and myoblasts. Native Col6, but not its pepsin-resistant fragment, counteracts the early differentiation of myogenic cells by reducing the expression of differentiation marker genes and preserving stemness features, with inhibition of the canonical Wnt pathway. Our data indicate that extracellular Col6 acts as a soluble ligand in delaying myogenic early differentiation by regulating intracellular signals involved in adult myogenesis.

Introduction

Satellite cells are the major pool of MuSCs involved in the growth and repair of skeletal muscle. Following muscle injury, MuSCs exit from quiescence and proliferate, providing new myoblasts which fuse each other and with pre-existent myofibers to regenerate the tissue (Bentzinger et al., 2013a). In the quiescent state, satellite cells reside in a specialized niche beneath the basal lamina and in close contact with myofiber sarcolemma (Yin et al., 2013). The MuSC niche is endowed with finely regulated biochemical and biomechanical properties which guarantee the maintenance of MuSC quiescence and, at the same time, guide the different steps of MuSC proliferation, activation and differentiation (Kuang et al., 2008). One major component of MuSC niche is the extracellular matrix (ECM), which significantly influences the environmental signals controlling MuSC function (Gattazzo et al., 2014; Loreti and Sacco, 2022). Several ECM proteins were found to influence MuSC function, including collagen VI (Col6), collagen V, fibronectin, laminin-211, laminin-111, fibrillin 1 and tenascin C, thus providing valuable information for dissecting the roles of ECM in muscle physiopathology (Bentzinger et al., 2013b; Urciuolo et al., 2013; Tierney et al., 2016; Baghdadi et al., 2018; Rayagiri et al., 2018).

Col6 is a large protein with a broad distribution in the ECM of different organs, including skin, muscles, tendons, blood vessels, joints and nerves (Cescon et al., 2015). Among ECM components, Col6 has a distinctive process of intracellular assembly made of several different steps. The process starts with the association of three genetically distinct polypeptide chains, α1(VI), α2(VI) and α3(VI), which form a triple-helical monomer (≈500 kDa) containing large N- and C-terminal globular domains and a relatively short collagenous stalk. Monomers then assemble into antiparallel dimers (≈1000 kDa) and tetramers (≈2000 kDa) that are finally secreted in the extracellular space, where they form a branched network of “beaded microfilaments” (Colombatti et al., 1987; Colombatti et al., 1995; Baldock et al., 2003). The key role of Col6 in skeletal muscle is underlined by the fact that its deficiency leads to muscle pathology in both humans and mice (Jöbsis et al., 1996; Irwin et al., 2003; Grumati et al., 2010). Mutations of *COL6A1-A3* genes are causative for Col6-related myopathies, inherited muscle disorders primarily characterized by muscle weakness and wasting, joint hyperlaxity and multiple contractures, and for which no cure is available yet (Bönnemann, 2011).

Within the MuSC niche, Col6 is expressed by quiescent satellite cells and by stromal cells, such as interstitial fibroblasts and fibro-adipogenic precursors, which are known to contribute to niche formation and remodeling (Zou et al., 2008; Urciuolo et al., 2013; Petrany et al., 2020). Col6 contribution for MuSC homeostasis and muscle regeneration was

highlighted by work in Col6 null mice, in which MuSCs are constitutively more activated and display lower self-renewal capability, linking these defects to altered biomechanical properties of the niche elicited by Col6 deficiency (Urciuolo et al., 2013). Yet, it is conceivable that Col6 may also convey important biochemical signals, given its ability to bind several surface receptors (Cescon et al., 2015; Tonelotto et al., 2021). Here, we investigated the effects exerted directly by Col6 on the *in vitro* differentiation of both C2C12 myogenic cells and primary MuSCs derived from wild-type mice. Our results show that Col6 delays the early differentiation of myogenic cells by maintaining them in a more stem condition via inhibition of the Wnt signaling pathway.

Results and discussion

Col6 inhibits early *in vitro* differentiation of C2C12 myoblasts

We first used the C2C12 myogenic cell line and assessed the capability of Col6 to modulate *in vitro* myogenic differentiation by culturing C2C12 cells in low serum for 48 hr, when expression of differentiation markers is markedly increased (Fig. S1A), and evaluating the effects elicited by increasing amounts of purified Col6 directly added to culture medium. Many commercially available collagen molecules are based on pepsin digestion of animal tissues, a procedure which preserves triple helical regions but detrimental for the integrity of the whole protein and respective interactors, especially for those collagens with extended non-triple helical regions, such as Col6. Therefore, we purified murine native Col6 with an *ad hoc* protocol and used it as soluble protein for *in vitro* treatments, in comparison with the pepsin-resistant Col6 fragment. After 48 hr of treatment, we detected a significantly decreased expression of *Myog, Acta1* and *Myh3* differentiation marker genes in cultures treated with full-length Col6 (Fig. 1A), but not in those treated with pepsin-resistant Col6, when compared to untreated controls (Fig. S1C). The Col6-mediated downregulation of myogenic differentiation genes was still maintained when cells were treated in the presence of inhibitory antibodies against β1 integrin, a known Col6 receptor binding the triple helical region (Pfaff et al., 1993), thus suggesting that such interaction is not required for the transduction of these effects (Fig. S1D). Cell attachment assays showed significantly delayed cell adhesion to fibronectin, a main extracellular ligand for β1 integrin, when C2C12 cells were treated with the same inhibitory antibody, confirming their inhibition of β1 integrin binding (Fig. S1E).

Col6 also elicited a significantly increased expression of Pax7 (Fig. S1D), a key transcription factor for SC stemness (von Maltzahn et al., 2013). To delve deeper into the

potential cell receptor(s) involved in the transduction of Col6 signals modulating myogenic differentiation, we used chemical inhibitors targeting different receptor classes for ECM ligands, including known cell surface interactors of Col6, such as RGD-dependent and RGD-independent integrins and discoidin domain receptors (DDR) 1 and 2. Interestingly, none of the applied inhibitors was effective in reducing the inhibitory effects produced by Col6 (Fig. S2A-C), thus implying that integrins and DDRs do not play substantial roles in mediating the differentiation inhibitory signals elicited by Col6 in C2C12 cells. The above findings were further supported by western blot and immunofluorescence experiments, showing a marked decrease of MyoG and MyH3 protein levels and of the percentage of MyH3-positive cells in C2C12 cultures treated with full-length Col6 (Fig. 1B; Fig. S1B and S2B,C).

Taken together, these results indicated that Col6 supplementation is able to counteract myoblast early differentiation, pointing at a role for Col6 in myogenesis. Therefore, we carried out further work aimed at establishing how Col6 regulates *in vitro* myogenesis, shifting our attention to primary MuSCs and the effects exerted by Col6 in the initial steps of MuSC differentiation.

Col6 delays *in vitro* MuSC differentiation by maintaining stemness properties

To explore the effects exerted by Col6 on MuSC differentiation, we first implemented an optimal *in vitro* experimental setup for such studies. Indeed, it is well known that when isolated from muscles and cultured *in vitro*, MuSCs lose their quiescent state and enter in a proliferating phase, therefore secreted factors regulating MuSC behavior in their niche, such as fibroblast growth factor 2 (FGF2), insulin-like growth factor, hepatocyte growth factor and activators of Notch signaling, are routinely used to sustain MuSC stemness and prevent spontaneous *in vitro* differentiation (Yin et al., 2013). We isolated satellite cells from wild-type mice and used them for establishing primary MuSC cultures. Withdrawal of FGF2 for 48 hr was sufficient to induce modification of cell shape, which became elongated and myoblast-like (Fig. 2A). FGF2 withdrawal also led to increased expression of myogenic differentiation genes, as well as to strong downregulation of tenascin C (*Tnc*) gene, known to promote MuSC stemness and self-renewal (Tierney et al., 2016) (Fig. 2B; Fig. S3A), thus confirming that differentiation was prompted. This was paralleled by a drop in proliferation rates, as illustrated by the decreased number of Ki-67-positive nuclei (Fig. S3B) and the increased MyH3 and MyoG protein levels following FGF2 withdrawal (Fig. 2C,D).

Based on these data, we used the same primary MuSC cultures and investigated the effects elicited by supplementation of Col6, or of collagen I (Col1) used as a control, upon

FGF2 withdrawal for 24 or 48 hr. Morphometric analysis of primary MuSC cultures under differentiating conditions revealed that Col6 administration inhibits cell elongation, as highlighted by a significant increase in the circularity index of Col6-treated cultures when compared to the corresponding untreated cultures (Fig. 3A,B). Notably, such increase was displayed by both 24 hr and 48 hr treatments with full-length Col6, and the circularity index was not significantly different from that of control cultures maintained in the presence of FGF2 (Fig. 3B). In agreement with this, the percentage of Pax7-positive cells, which as expected was high in the presence of FGF2 and dramatically decreased upon FG2 withdrawal, was partially restored by Col6 treatment but not by Col1 treatment (Fig. 3C,D), thus highlighting the capability of Col6 to maintain a higher stemness rate even in the absence of FGF2. This conclusion was also supported by the expression of myogenic markers, showing significantly decreased levels of *Myh3*, *Myog* and *Acta1* transcripts (Fig. 3E) and of MyH3 and MyoG proteins (Fig. 3F) in Col6-treated cultures. Intriguingly, cultures treated with Col1 displayed an opposite effect, with significantly higher levels of *Myog* and *Myod* transcripts than untreated cultures (Fig. 3E). Furthermore, the stemness markers syndecan-3 and tenascin C (Pisconti et al., 2016; Tierney et al., 2016) showed significantly higher expression levels in Col6-treated cultures when compared to the corresponding untreated cultures (Fig. S3C).

This set of data showed that soluble Col6 counteracts early *in vitro* differentiation of MuSCs, maintaining them in a less differentiated state. These findings strengthen the concept that Col6 is a critical regulator of MuSC stemness, revealing that beside a fine regulation of the mechanical properties of MuSC niche exerted through the branched network of Col6 microfilaments deposited in the ECM (Urciuolo et al., 2013), native Col6 is capable to delay early myogenic differentiation in a stiffness-independent fashion.

Col6 treatment negatively regulates canonical Wnt signaling

The maintenance of MuSC stemness is strictly regulated by a balance between Notch and Wnt signaling pathways, in which the first favors dormancy (Bi et al., 2016; Baghdadi et al., 2018) while the second promotes myogenic differentiation (Brack et al., 2008; Brack et al., 2009). Therefore, we explored whether the Col6-dependent effects on *in vitro* MuSC differentiation relies on the modulation of these pathways. We first assessed the subcellular localization of β-catenin, the major transcriptional coactivator of canonical Wnt pathway. Immunofluorescence and western blotting showed that treatment of differentiating MuSC cultures with full-length Col6 significantly decreases the amount of nuclear β-catenin (Fig. 4A) as well as β-catenin total protein levels (Fig. 4B). As expected, treatment with Wnt-3a,

used as a positive control, led to a distinct nuclear localization of β-catenin in differentiating SC-derived cultures (Fig. S4A). We next assessed the activation state of glycogen synthase kinase 3 (GSK-3), a negative regulator of Wnt signaling targeting β-catenin for degradation, and found a significant decrease of the inhibitory phosphorylation of GSK-3β in Col6-treated cultures when compared to the corresponding control cultures (Fig. 4B), pointing to down-regulation of the Wnt pathway.

To corroborate these findings, we analyzed the expression of prospero-related homeobox 1 (Prox1), a transcription factor playing an essential role for MuSC differentiation and whose activity is strictly regulated by the Wnt/β-catenin pathway (Kivelä et al., 2016). Expression of *Prox1* gene was strongly upregulated in MuSC cultures upon FGF2 withdrawal, in agreement with its role in promoting myogenic differentiation (Fig. S4B). Col6 treatment led to a significant decrease of *Prox1* expression in differentiating MuSCs (Fig. S4C), again supporting the concept that the effects elicited by Col6 supplementation involve modulation of the Wnt/β-catenin pathway. On the other hand, the Col6-dependent effects in enhancing stemness and delaying differentiation of primary MuSC cultures do not appear to primarily involve the Notch signaling pathway, at least in this experimental setup. Indeed, the expression levels of several major Notch target genes (such as *Notch2, Notch3, Eya1, Hes1, Hey1* and *Heyl*) were not significantly different between Col6-treated and untreated control cultures maintained under the same differentiating conditions as above (Fig. 4C), pointing at a marginal or absent involvement of this pathway in the effects elicited by Col6. Taken together, the above set of data revealed that Col6 treatment of differentiating MuSC cultures inhibits the Wnt/β-catenin pathway, leading in turn to decreased differentiation and higher maintenance of the stemness state.

In conclusion, these results provide new information on the mechanisms involved in stem cell-niche interactions, offering some novel concepts about the diverse roles of Col6 in skeletal muscle, as well as for muscle homeostasis and regeneration. Future work aimed at the use of native Col6 and its various domains with different *in vitro* and *ex vivo* models and experimental setups will allow throwing light on the Col6 subregions involved in the effects exerted by this key ECM molecule in the different muscle cell types, also giving a boost for the identification of surface receptors and ligands involved in the transduction of outside-in signals triggered by Col6 in myofibers, satellite cells and stromal cells, an essential step for the development of targeted therapeutic strategies in Col6-related myopathies and other muscle disorders.

Materials and methods

Satellite cell isolation and primary MuSC cultures. Satellite cells were isolated from the extensor digitorum longus muscle of 1- to 2-month-old wild-type mice of the C57/BL6N strain. Muscles were cleared from tendons and fat tissue, and then chopped with scissors and scalpel. The obtained specimens were chemically digested twice with 15 ml phosphate buffer saline (PBS) supplemented with collagenase I (100 U/ml, Worthington, Lakewood, NJ, USA) and dispase (2 U/ml, Thermo Fisher Scientific, Waltham, MA, USA) for 20 min at 37° C in agitation. The solution was filtered through a 70-µm cell strainer to eliminate residues of muscle debris and then centrifuged at 1600 rpm for 30 min. The cell pellet was resuspended in Dulbecco's Modified Eagle's Medium (DMEM, Thermo Fisher Scientific) supplemented with 20% fetal bovine serum (FBS, Thermo Fisher Scientific) and plated onto 0.1% gelatin-precoated dishes for 1 hr at 37° C in 5% CO_2, to deplete muscle fibroblasts and other cells. Following this pre-plating step, cells remaining in suspension were plated onto 0.1% gelatin-precoated dishes and cultured in DMEM medium supplemented with 20% FBS, 1% glutamine (Thermo Fisher Scientific), 1% penicillin/streptomycin (Thermo Fisher Scientific) and 5% chicken embryo extract (Life Science Production, Bedford, UK) at 37° C in 5% CO_2. After the first passage, MuSCs were cultured in Ham's F-10 medium (Thermo Fisher Scientific) supplemented with 10% FBS, 1% glutamine, 1% penicillin/streptomycin and 25 ng/ml recombinant FGF2 (Wellcome-MRC Cambridge Stem Cell Institute, Cambridge, UK), to maintain them in a stem and proliferating condition. Differentiation was induced by FG2 withdrawal and culture in the same medium as above. Only second to fourth passages from initial isolation were used for all the experiments. Primary MuSCs preparations that were minorly contaminated by muscle fibroblast were discarded and not used.

C2C12 cells. C2C12 (CRL-1772; ATCC, Manassas, VA, USA) cells were used as an immortalized murine myogenic cell line, and cultured in DMEM medium supplemented with 20% FBS, 1% glutamine and 1% penicillin/streptomycin at 37° C in 5% CO_2. To induce myoblast differentiation and fusion, C2C12 were cultured for 2 days in DMEM medium supplemented with 2% horse serum, 1% glutamine and 1% penicillin/streptomycin at 37° C in 5% CO_2. Both C2C12 and primary SC cultures were routinely tested for mycoplasma contamination and visually inspected for morphology and signs of bacterial contamination.

Cell treatments. The triple helical pepsin-resistant fragment of Col6 was purified from mouse tissues by pepsin digestion, fractionated salt precipitation and molecular sieve chromatography, as previously described (Trüeb et al., 1987; Bonaldo et al., 1998). Native full-length Col6 (whole tetrameric molecule) was purified from newborn wild-type mice by fractionated salt precipitation and molecular sieve chromatography, following established

procedures and as previously described (Colombatti et al., 1989; Sabatelli et al., 2001). Both preparations were tested for purity by ELISA and SDS-PAGE gel electrophoresis. Col1 was purchased from Sigma-Aldrich. Cells were treated with either full-length Col6, pepsin-resistant Col6 fragment, or Col1, added as soluble molecules to culture medium. Inhibitory antibodies against β1 integrin (rabbit monoclonal; Epitomics, Burlingame, CA, USA) were used at 10 µg/ml in culture medium. For cell attachment assays, C2C12 cells were preincubated with 10 µg/ml β1 integrin inhibitory antibody for 30 min in culture medium before plating them onto dishes coated with fibronectin (5 µg/cm^2), and images taken at 5, 10, 15, 30 and 90 min after plating. For treatments with chemical inhibitors, C2C12 cells were maintained for 2 days in culture medium supplemented with the following compounds: TC-I 15 (100 µM; Tocris Bioscience, Bristol, UK), RGDS peptide (100 µM; Tocris Bioscience), RGES peptide (100 µM; Abbexa, Cambridge, UK), 7rh (20 nM; Tocris Bioscience) and WRG-28 (300 nM; Tocris Bioscience). Where indicated, SCs were treated with 10 ng/ml recombinant murine Wnt-3a (Peprotech, Cranbury, NJ, USA) for 48 hr in differentiation medium.

Quantitative real-time RT-PCR (RT-qPCR). Total RNA was extracted from cell samples using 0.5 ml TRIzol Reagent (Thermo Fisher Scientific) and quantified with Nanodrop ND-1000 (NanoDrop Technologies, Wilmington, DE, USA). Reverse transcription was performed with 500 ng total RNA and M-MLV Reverse Transcriptase (Thermo Fisher Scientific), using random hexamers as previously described (Da Ros et al., 2022). The resulting cDNAs were processed for quantitative real-time PCR using Rotor-Gene SYBR Green PCR Kit mastermix (Qiagen, Hilden, Germany) and a Rotor-GeneQ thermocycler (Qiagen). Each sample was loaded in triplicate and analyzed with RotorGene Q 2.0.24 software. *Rps16*, coding for ribosomal protein S16, was used as a housekeeping gene control. Primer sequences are provided in Table S1.

Western blotting. C2C12 and primary MuSCs were lysed in RIPA buffer (20 mM Tris-HCl, pH 7.5, 150 mM NaCl, 1 mM EGTA, 1% NP-40, 1% sodium deoxycholate) supplemented with protease and phosphatase inhibitors (Sigma-Aldrich, Saint Louis, MO, USA) and stored at -80° C until use. Protein concentration was determined by the BCA Protein Assay Kit (Thermo Fisher Scientific) and 30-40 µg of protein samples were subjected to SDS-PAGE in polyacrylamide Novex NuPAGE Bis-Tris 4-12% gels (Thermo Fisher Scientific), followed by electrotransfer onto polyvinylidene difluoride membranes (Millipore) as previously described (Metti et al., 2020). Membranes were stained with Ponceau (Sigma-Aldrich) and blocked for 1 hr with 5% non-fat dry milk (Bio-Rad, Hercules, CA, USA) in Tris-buffered saline solution

containing 0.1% Tween 20 (TBS-T), and then incubated overnight at 4° C with the primary antibodies as previously described (Gambarotto et al., 2022). The following primary antibodies were used: mouse monoclonal anti-MyH3 (1:500, Developmental Studies Hybridoma Bank, Iowa City, IA, USA); mouse monoclonal anti-MyoG (1:300, Santa Cruz Biotechnology, Dallas, TX, USA); rabbit polyclonal anti-phospo-GSK-3α/β (Ser 21/9) (1:1000, Cell Signaling Technology, Danvers, MA, USA); rabbit monoclonal anti-β-catenin (1:500, Abcam, Cambridge, UK); mouse monoclonal anti-β-actin (1:3000, Sigma-Aldrich). After three washes in TBS-T, membranes were incubated for 1 hr with horseradish peroxidase-conjugated anti-rabbit or anti-mouse secondary antibodies (1:1000; Bethyl Laboratories, Montgomery, TX, USA). Detection was carried out by SuperSignal West Pico (Thermo Fisher Scientific). Densitometric quantification was performed by Fiji software (Rueden et al., 2017). Uncropped gels used in the figures are displayed in supplementary material for blot transparency (Figure S5).

Immunofluorescence. For immunofluorescence analyses, C2C12 cells were plated in 24-well plates on glass coverslips, whereas primary MuSCs were cultivated in 8-well chamber slides (Thermo Fisher Scientific). Cells were fixed with 4% paraformaldehyde at room temperature for 2 min and washed three times in PBS for 5 min. Permeabilization was performed using cold (-20° C) methanol for 5 min for C2C12 cells or 0.3% Triton X-100 in PBS for 10 min for primary MuSCs. Slides were washed three times in PBS and then incubated for 1 hr with 10% goat serum in PBS, to block unspecific binding of antibodies. Primary antibodies against Pax7 (1:25; mouse monoclonal; Developmental Studies Hybridoma Bank), MyoG (1:200; rabbit monoclonal; Abcam), MyH3 (1:200; mouse monoclonal; Developmental Studies Hybridoma Bank), Ki67 (1:100; rabbit monoclonal; Novus Biologicals, Centennial, CO, USA) and β-catenin (1:200; rabbit polyclonal; Abcam) were diluted in 5% goat serum in PBS and incubated at 4° C overnight in a humidified chamber. Slides were washed three times in PBS and incubated for 1 hr with anti-rabbit Cy2 or Cy3 (1:500; Jackson ImmunoResearch, West Grove, PA, USA) and anti-mouse Cy3 (1:500; Jackson ImmunoResearch) secondary antibodies. Nuclei were counterstained with Hoechst 33258 (Sigma-Aldrich). After three washes in PBS, slides were finally mounted in 80% glycerol in PBS.

Morphometric analysis. Bright-field micrographs were captured with a Leica DMI4000 inverted microscope at 10x magnification, and the circularity index was calculated using FIJI

software, by setting a range extending from 0 (highly elongated shape) to 1 (circular shape) (Rueden et al., 2017; Eliazer et al., 2019).

Statistics. All results are shown as mean ± s.e.m. Statistical analysis of data was performed by unpaired two-tailed Mann-Whitney test (GraphPad), except where indicated. For experiments with more than two conditions, one-way or two-way analysis of variant (ANOVA) was used (GraphPad). When ANOVA revealed significant differences, further analysis was carried out using Holm-Sidak's multiple comparison test. Statistical significance was set at P <0.05. All histograms display individual values, and the number of biological replicates (always greater than three) is indicated in the figures' captions.

Acknowledgements

We thank all the members of Bonaldo's lab for helpful discussions and suggestions.

Competing interests

The authors declare no competing of financial interests.

Author contributions

Conceptualization: S.M., F.D.R., P.B.; Methodology: S.M., F.D.R.; Validation: S.M., F.D.R.; Formal analysis: S.M., F.D.R., M.C.; Investigation: S.M., F.D.R., G.T., M.C.; Resources: P.B.; Data curation: S.M., F.D.R.; Writing - original draft: S.M., F.D.R., P.B.; Writing - review & editing: S.M., F.D.R., P.B.; Supervision: F.D.R., M.C., P.B.; Project administration: M.C., P.B.; Funding acquisition: P.B.

Funding

This work was supported by grants from the Italian Ministry of Education, University and Research (Grants 201742SBXA and 2022MXH3JY), Telethon Foundation (Grant GGP19229) and University of Padova.

References

Baghdadi, M. B., Castel, D., Machado, L., Fukada, S. I., Birk, D. E., Relaix, F., Tajbakhsh, S. and Mourikis, P. (2018). Reciprocal signalling by Notch-Collagen V-CALCR retains muscle stem cells in their niche. *Nature* **557**, 714-718. https://doi.org/10.1038/s41586-018-0144-9

Baldock, C., Sherratt, M. J., Shuttleworth, C. A. and Kielty, C. M. (2003). The supramolecular organization of collagen VI microfibrils. *J. Mol. Biol.* **330**, 297-307. https://doi.org/10.1016/s0022-2836(03)00585-0

Bentzinger, C. F., Wang, Y. X., Dumont, N. A. and Rudnicki, M. A. (2013a). Cellular dynamics in the muscle satellite cell niche. *EMBO Rep.* **14**, 1062-1072. https://doi.org/10.1038/embor.2013.182

Bentzinger, C. F., Wang, Y. X., von Maltzahn, J., Soleimani, V. D., Yin, H. and Rudnicki, M. A. (2013b). Fibronectin regulates Wnt7a signaling and satellite cell expansion. *Cell Stem Cell* **12**, 75-87. https://doi.org/10.1016/j.stem.2012.09.015

Bi, P., Yue, F., Sato, Y., Wirbisky, S., Liu, W., Shan, T., Wen, Y., Zhou, D., Freeman, J. and Kuang, S. (2016). Stage-specific effects of Notch activation during skeletal myogenesis. *Elife* **5**, e17355. https://doi.org/10.7554/elife.17355

Bönnemann, C. G. (2011). The collagen VI-related myopathies: muscle meets its matrix. *Nat. Rev. Neurol.* **7**, 379-390. https://doi.org/10.1038/nrneurol.2011.81

Bonaldo, P., Braghetta, P., Zanetti, M., Piccolo, S., Volpin, D. and Bressan, G. M. (1998). Collagen VI deficiency induces early onset myopathy in the mouse: an animal model for Bethlem myopathy. *Hum. Mol. Genet.* **7**, 2135-2140. https://doi.org/10.1093/hmg/7.13.2135

Brack, A. S., Conboy, I. M., Conboy, M. J., Shen, J. and Rando, T. A. (2008). A temporal Switch from Notch to Wnt signaling in muscle stem cells is necessary for normal adult myogenesis. *Cell Stem Cell* **2**, 50-59. https://doi.org/10.1016/j.stem.2007.10.006

Brack, A. S., Murphy-Seiler, F., Hanifi, J., Deka, J., Eyckerman, S., Keller, C., Aguet, M. and Rando, T. A. (2009). BCL9 is an essential component of canonical Wnt signaling that mediates the differentiation of myogenic progenitors during muscle regeneration. *Dev. Biol.* **335**, 93-105. https://doi.org/10.1016/j.ydbio.2009.08.014

Cescon, M., Gattazzo, F., Chen, P. and Bonaldo, P. (2015). Collagen VI at a glance. *J. Cell. Sci.* **128**, 3525-3531. https://doi.org/10.1242/jcs.169748

Colombatti, A., Ainger, K. and Colizzi, F. (1989). Type VI collagen: high yields of a molecule with multiple forms of alpha 3 chain from avian and human tissues. *Matrix* **9**, 177-185. https://doi.org/10.1016/S0934-8832(89)80048-4

Colombatti, A., Bonaldo, P., Ainger, K., Bressan, G. M. and Volpin, D. (1987). Biosynthesis of chick type VI collagen. I. Intracellular assembly and molecular structure. *J. Biol. Chem.* **262**, 14454-14460. https://doi.org/10.1016/s0021-9258(18)47816-7

Colombatti, A., Mucignat, M. T. and Bonaldo, P. (1995). Secretion and matrix assembly of recombinant type VI collagen. *J. Biol. Chem.* **270**, 13105-13111. https://doi.org/10.1074/jbc.270.22.13105

Da Ros, F., Persano, L., Bizzotto, D., Michieli, M., Braghetta, P., Mazzucato, M. and Bonaldo, P. (2022). Emilin-2 is a component of bone marrow extracellular matrix regulating mesenchymal stem cell differentiation and hematopoietic progenitors. *Stem Cell Res. Ther.* **13**, 2. https://doi.org/10.1186/S13287-021-02674-2

Eliazer, S., Muncie, J. M., Christensen, J., Sun, X., D'Urso, R. S., Weaver, V. M. and Brack, A. S. (2019). Wnt4 from the niche controls the mechano-properties and quiescent state of muscle stem cells. *Cell Stem Cell* **25**, 654-665. https://doi.org/10.1016/j.stem.2019.08.007

Gambarotto, L., Metti, S., Chrisam, M., Cerqua, C., Sabatelli, P., Armani, A., Zanon, C., Spizzotin, M., Castagnaro, S., Strappazzon, F. et al. (2022). Ambra1 deficiency impairs mitophagy in skeletal muscle. *J. Cachexia Sarcopenia Muscle* **13**, 2211-2224. https://doi.org/10.1002/jcsm.13010

Gattazzo, F., Urciuolo, A. and Bonaldo, P. (2014). Extracellular matrix: A dynamic microenvironment for stem cell niche. *Biochim. Biophys. Acta* **1840**, 2506-2519. https://doi.org/10.1016/j.bbagen.2014.01.010

Grumati, P., Coletto, L., Sabatelli, P., Cescon, M., Angelin, A., Bertaggia, E., Blaauw, B., Urciuolo, A., Tiepolo, T., Merlini, L. et al. (2010). Autophagy is defective in collagen VI muscular dystrophies, and its reactivation rescues myofiber degeneration. *Nat. Med.* **16**, 1313-1320. https://doi.org/10.1038/nm.2247

Irwin, W. A., Bergamin, N., Sabatelli, P., Reggiani, C., Megighian, A., Merlini, L., Braghetta, P., Columbaro, M., Volpin, D., Bressan, G. M. et al. (2003). Mitochondrial dysfunction and apoptosis in myopathic mice with collagen VI deficiency. *Nat. Genet.* **35**, 367-371. https://doi.org/10.1038/ng1270

Jöbsis, G. J., Keizers, H., Vreijling, J. P., de Visser, M., Speer, M. C., Wolterman, R. A., Baas, F. and Bolhuis, P. A. (1996). Type VI collagen mutations in Bethlem myopathy, an autosomal dominant myopathy with contractures. *Nat. Genet.* **14**, 113-115. https://doi.org/10.1038/ng0996-113

Kivelä, R., Salmela, I., Nguyen, Y. H., Petrova, T. V., Koistinen, H. A., Wiener, Z. and Alitalo, K. (2016). The transcription factor Prox1 is essential for satellite cell differentiation and muscle fibre-type regulation. *Nat. Commun.* **7**, 13124. https://doi.org/10.1038/ncomms13124

Kuang, S., Gillespie, M. A. and Rudnicki, M. A. (2008). Niche regulation of muscle satellite cell self-renewal and differentiation. *Cell Stem Cell* **2**, 22-31. https://doi.org/10.1016/j.stem.2007.12.012

Loreti, M. and Sacco, A. (2022). The jam session between muscle stem cells and the extracellular matrix in the tissue microenvironment. *NPJ Regen. Med.* **7**, 1-15. https://doi.org/10.1038/s41536-022-00204-z

Metti, S., Gambarotto, L., Chrisam, M., Baraldo, M., Braghetta, P., Blaauw, B. and Bonaldo, P. (2020). The polyphenol pterostilbene ameliorates the myopathic phenotype of collagen VI deficient mice via autophagy induction. *Front. Cell. Dev. Biol.* **8**, 580933. https://doi.org/10.3389/fcell.2020.580933

Petrany, M. J., Swoboda, C. O., Sun, C., Chetal, K., Chen, X., Weirauch, M. T., Salomonis, N. and Millay, D. P. (2020). Single-nucleus RNA-seq identifies transcriptional heterogeneity in multinucleated skeletal myofibers. *Nat. Commun.* **11**, 1-12. https://doi.org/10.1038/s41467-020-20063-w

Pfaff, M., Aumailley, M., Specks, U., Knolle, J., Zerwes, H. G. and Timpl, R. (1993). Integrin and Arg-Gly-Asp dependence of cell adhesion to the native and unfolded triple helix of collagen type VI. *Exp. Cell Res.* **206**, 167-176. https://doi.org/10.1006/excr.1993.1134

Pisconti, A., Banks, G. B., Babaeijandaghi, F., Betta, N. D., Rossi, F. M. V., Chamberlain, J. S. and Olwin, B. B. (2016). Loss of niche-satellite cell interactions in syndecan-3 null mice alters muscle progenitor cell, improving muscle regeneration. *Skelet. Muscle* **6**, 1-14. https://doi.org/10.1186/s13395-016-0104-8

Rayagiri, S. S., Ranaldi, D., Raven, A., Mohamad Azhar, N. I. F., Lefebvre, O., Zammit, P. S. and Borycki, A.G. (2018). Basal lamina remodeling at the skeletal muscle stem cell niche mediates stem cell self-renewal. *Nat. Commun.* **9***,* 1075. https://doi.org/10.1038/s41467-018-03425-3

Rueden, C. T., Schindelin, J., Hiner, M. C., De Zonia, B. E., Walter, A. E., Arena, E. T. and Eliceiri, K. W. (2017). ImageJ2: ImageJ for the next generation of scientific image data. *BMC Bioinform.* **18**, 529. https://doi.org/10.1186/S12859-017-1934-Z

Sabatelli, P., Bonaldo, P., Lattanzi, G., Braghetta, P., Bergamin, N., Capanni, C., Mattioli, E., Columbaro, M., Ognibene, A., Pepe, G. et al. (2001). Collagen VI deficiency affects the organization of fibronectin in the extracellular matrix of cultured fibroblasts. *Matrix Biol.* **20**, 475-486. https://doi.org/10.1016/s0945-053x(01)00160-3

Tierney, M. T., Gromova, A., Sesillo, F. B., Sala, D., Spenlé, C., Orend, G. and Sacco, A. (2016). Autonomous extracellular matrix remodeling controls a progressive adaptation in muscle stem cell regenerative capacity during development. *Cell Rep.* **14**, 1940-1952. https://doi.org/10.1016/j.celrep.2016.01.072

Tonelotto, V., Castagnaro, S., Cescon, M. and Bonaldo, P. (2021). Collagens and muscle diseases: a focus on collagen VI. In *The Collagen Superfamily and Collagenopathies. Biology of Extracellular Matrix* (ed. F. Ruggiero). pp. 199-256. Cham, Switzerland: Springer International Publishing. https://dx.doi.org/10.1007/978-3-030-67592-9_6

Trüeb, B., Schreier, T., Bruckner, P. and Winterhalter, K. H. (1987). Type VI collagen represents a major fraction of connective tissue collagens. *Eur. J. Biochem.* **166**, 699-703. https://doi.org/10.1111/j.1432-1033.1987.tb13568.x

Urciuolo, A., Quarta, M., Morbidoni, V., Gattazzo, F., Molon, S., Grumati, P., Montemurro, F., Tedesco, F. S., Blaauw, B., Cossu, G. et al. (2013). Collagen VI regulates satellite cell self-renewal and muscle regeneration. *Nat. Commun.* **4**, 1964. https://doi.org/10.1038/NCOMMS2964

von Maltzahn, J., Jones, A. E., Parks, R. J. and Rudnicki, M. A. (2013). Pax7 is critical for the normal function of satellite cells in adult skeletal muscle. *Proc. Natl. Acad. Sci. USA* **110**, 16474-16479. https://doi.org/10.1073/pnas.1307680110

Yin, H., Price, F. and Rudnicki, M. A. (2013). Satellite cells and the muscle stem cell niche. *Physiol. Rev.* **93**, 23-67. https://doi.org/10.1152/physrev.00043.2011

Zou, Y., Zhang, R. Z., Sabatelli, P., Chu, M. L. and Bönnemann, C. G. (2008). Muscle interstitial fibroblasts are the main source of collagen VI synthesis in skeletal muscle: implications for congenital muscular dystrophy types Ullrich and Bethlem. *J. Neuropathol. Exp. Neurol.* **67**, 144-154. https://doi.org/10.1097/nen.0b013e3181634ef7

Figures

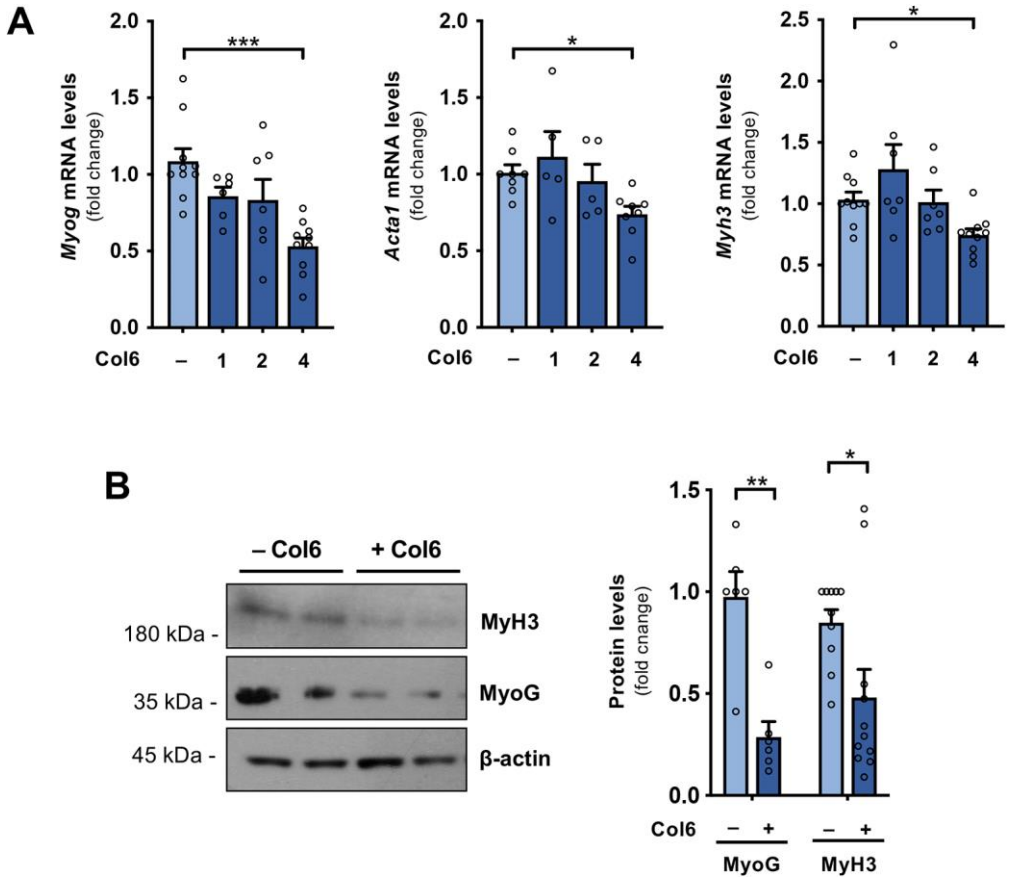

Fig. 1. Col6 inhibits *in vitro* differentiation of C2C12 myoblasts. (**A**) RT-qPCR analysis of *Myog, Acta1* and *Myh3* mRNA levels in C2C12 cells maintained for 48 hr in differentiating conditions (2% horse serum) in the absence of any treatment (–), or treated with different concentrations of soluble full-length Col6 (1, 2 and 4 µg/ml). mRNA levels are shown as fold change compared to the untreated condition (*n*=5-10, each condition; *, *P*<0.05; ***, *P*<0.001). (**B**) Representative western blot for MyH3 and MyoG protein levels in differentiating C2C12 cells maintained for 48 hr in the absence (–) or in the presence (+) of 4 µg/ml Col6. β-actin was used as loading control. Histograms on the right show the relative densitometric quantifications, as obtained from three independent western blot experiments (*n*=6-10, each condition; *, *P*<0.05; **, *P*<0.01).

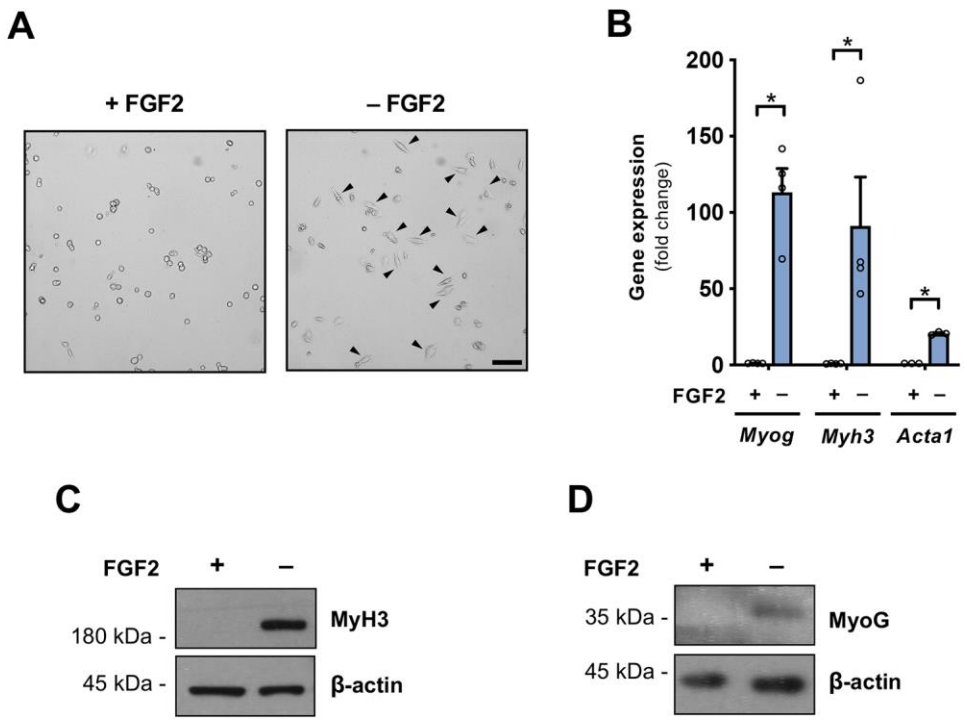

Fig. 2. Characterization of satellite cell-derived cultures of primary mouse MuSCs. (**A**) Representative bright-field images of MuSCs isolated from wild-type mice and cultured for 48 hr in the presence (+) or absence (–) of 25 ng/ml FGF2. Arrowheads point at differentiating cells with elongated, myoblast-like shape. Scale bar, 100 µm. (**B**) Gene expression analysis for myogenic differentiation markers, as determined by RT-qPCR of primary MuSCs cultured for 48 hr in the presence (+) or absence (–) of 25 ng/ml FGF2. mRNA levels are shown as fold change compared to the respective condition (*n*=3-4, each condition; *, *P*<0.05). (**C,D**) Representative western blot for MyH3 (**C**) and MyoG (**D**) in protein extracts of primary MuSCs cultured for 48 hr in the presence (+) or absence (–) of 25 ng/ml FGF2. β-actin was used as loading control.

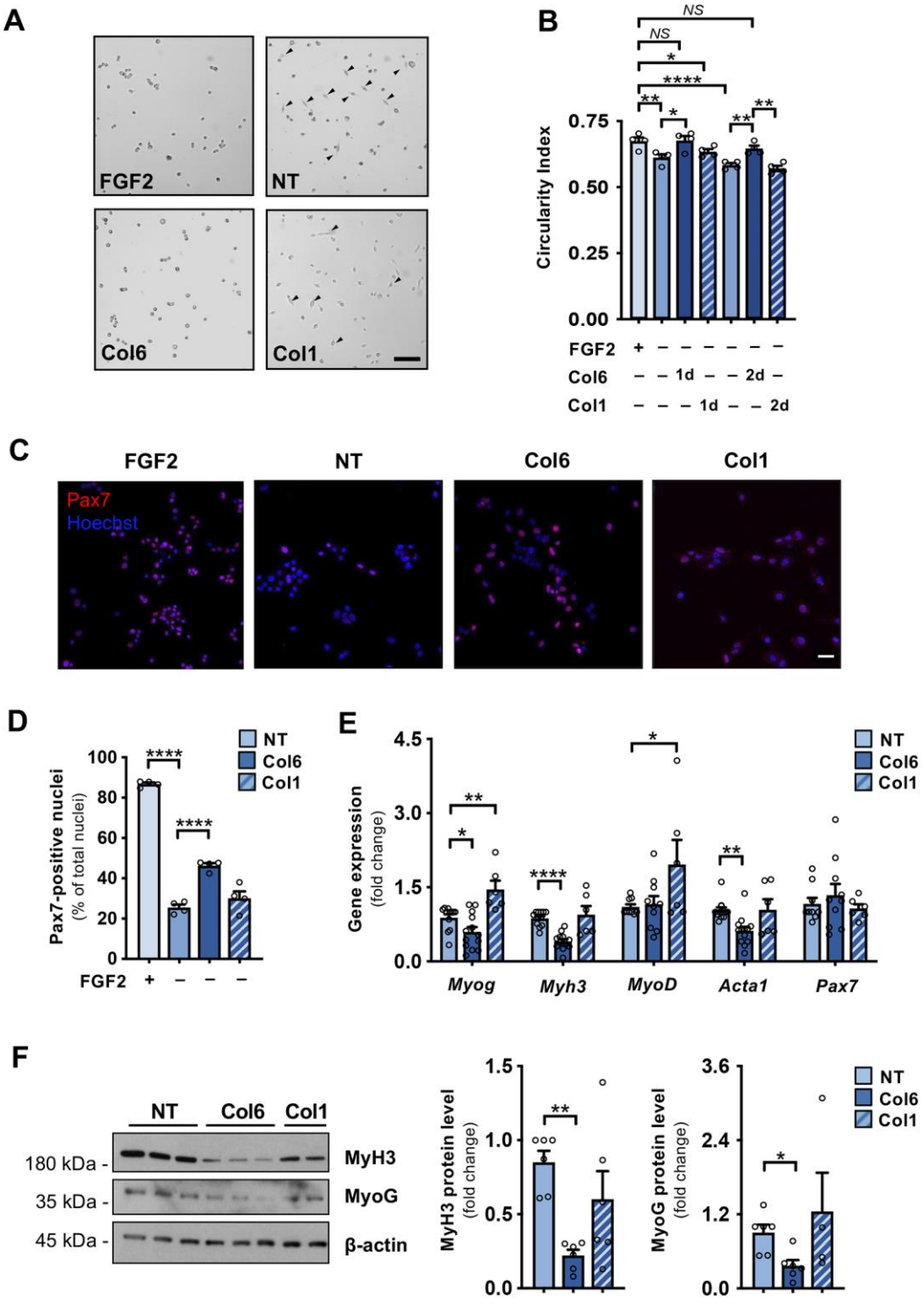

Fig. 3. Col6 delays *in vitro* MuSC differentiation and sustains stemness. (**A**) Representative bright-field images of primary differentiating MuSCs cultured for 48 hr under FGF2 withdrawal conditions in the absence (NT) or presence of 4 µg/ml Col6 or 4 µg/ml Col1. Arrowheads point at differentiating cells with elongated, myoblast-like shape. Scale bar, 100 µm. (**B**) Morphometric analysis of primary MuSCs cultured for 48 hr in the presence or absence of 25 ng/ml FGF2 and maintained without Col6

or treated with 4 µg/ml Col6 or 4 µg/ml Col1 for 24 hr (1d) or 48 hr (2d). The circularity indexes range from 0 (highly elongated shape) to 1 (fully circular shape) (*n*=4, each condition; **, *P*<0.01; ****, *P*<0.0001; NS, not significant). (**C**) Representative immunofluorescence for Pax7 (red) in primary MuSCs maintained for 48 hr in the presence of 25 ng/ml FGF2 (FGF2), or in the absence of FGF2 without any treatment (NT), or in the absence of FGF2 and treated with either 4 µg/ml Col6 or 4 µg/ml Col1. Nuclei were counterstained with Hoechst (blue). Scale bar, 50 µm. (**D**) Quantification of Pax7-positive cells vs total cells in primary MuSCs cultured for 48 hr in the presence (+) or absence (–) of 25 ng/ml FGF2 without any treatment (NT) or treated with 4 µg/ml Col6 or 4 µg/ml Col1 (*n*=4, each condition; ****, *P*<0.0001). (**E**) Gene expression analysis for myogenic differentiation (*Myog*, *Myh3*, *Myod*, *Acta1*) and stemness (*Pax7*) markers, as determined by RT-qPCR of primary MuSCs maintained for 48 hr in the absence of FGF2 and without any treatment (NT) or treated with either 4 µg/ml Col6 or 4 µg/ml Col1. mRNA levels are shown as fold change compared to the respective untreated condition (*n*=6-12, each condition; *, *P*<0.05; **, *P*<0.01; ****, *P*<0.0001). (**F**) Representative western blot for MyH3 and MyoG in protein extracts of primary MuSCs maintained for 48 hr in the absence of FGF2 and without any treatment (NT) or treated with either 4 µg/ml Col6 or 4 µg/ml Col1. β-actin was used as loading control. Histograms on the right show the relative densitometric quantifications, as obtained from three independent western blot experiments (*n*=4-6, each condition; *, *P*<0.05; **, *P*<0.01).

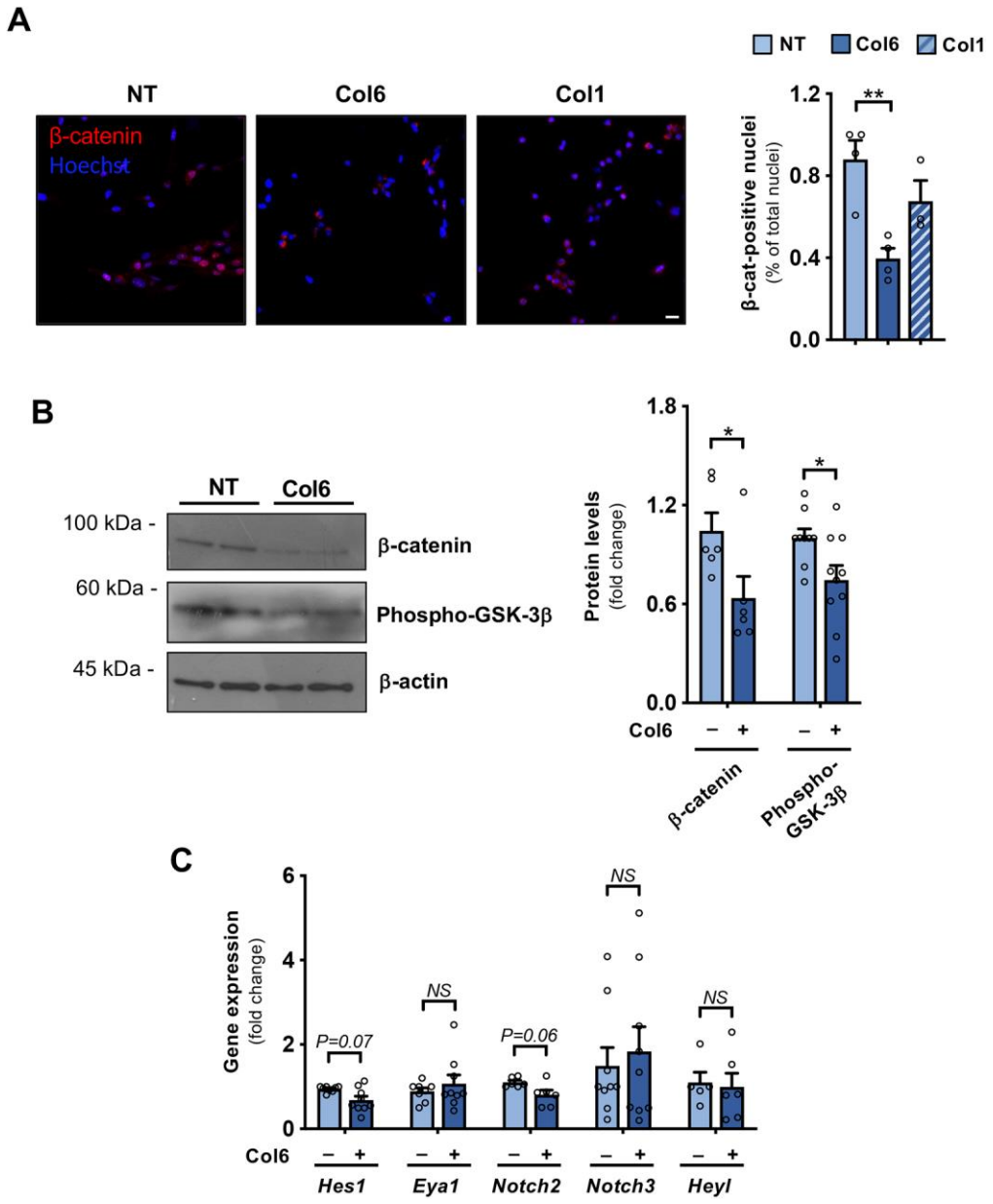

Fig. 4. Col6 treatment inhibits Wnt signaling without any significant induction of Notch signaling. (**A**) Representative immunofluorescence for β-catenin (red) in primary MuSCs maintained for 48 hr in the absence of FGF2 and without any treatment (NT) or treated with either 4 µg/ml Col6 or 4 µg/ml Col1. Nuclei were counterstained with Hoechst (blue). Scale bar, 50 µm. Histograms on the right show the quantification of β-catenin-positive nuclei vs total nuclei (*n*=3-4, each condition; **, *P*<0.01). (**B**) Representative western blotting for β-catenin and phospho-GSK-3β protein levels in primary MuSCs maintained for 48 hr in the absence of FGF2 without any treatment (NT) or treated with 4 µg/ml Col6. β-actin was used as loading control. Histograms on the right show the relative densitometric quantifications, as obtained

from three independent western blot experiments (*n*=6-9, each condition; *, *P*<0.05). (**C**) Gene expression analysis of Notch downstream targets, as determined by RT-qPCR of primary MuSCs maintained for 48 hr under FGF2 withdrawal in the absence (–) or presence (+) of 4 µg/ml Col6. mRNA levels are shown as fold change compared to the respective untreated condition (*n*=5-9, each condition; NS, not significant).

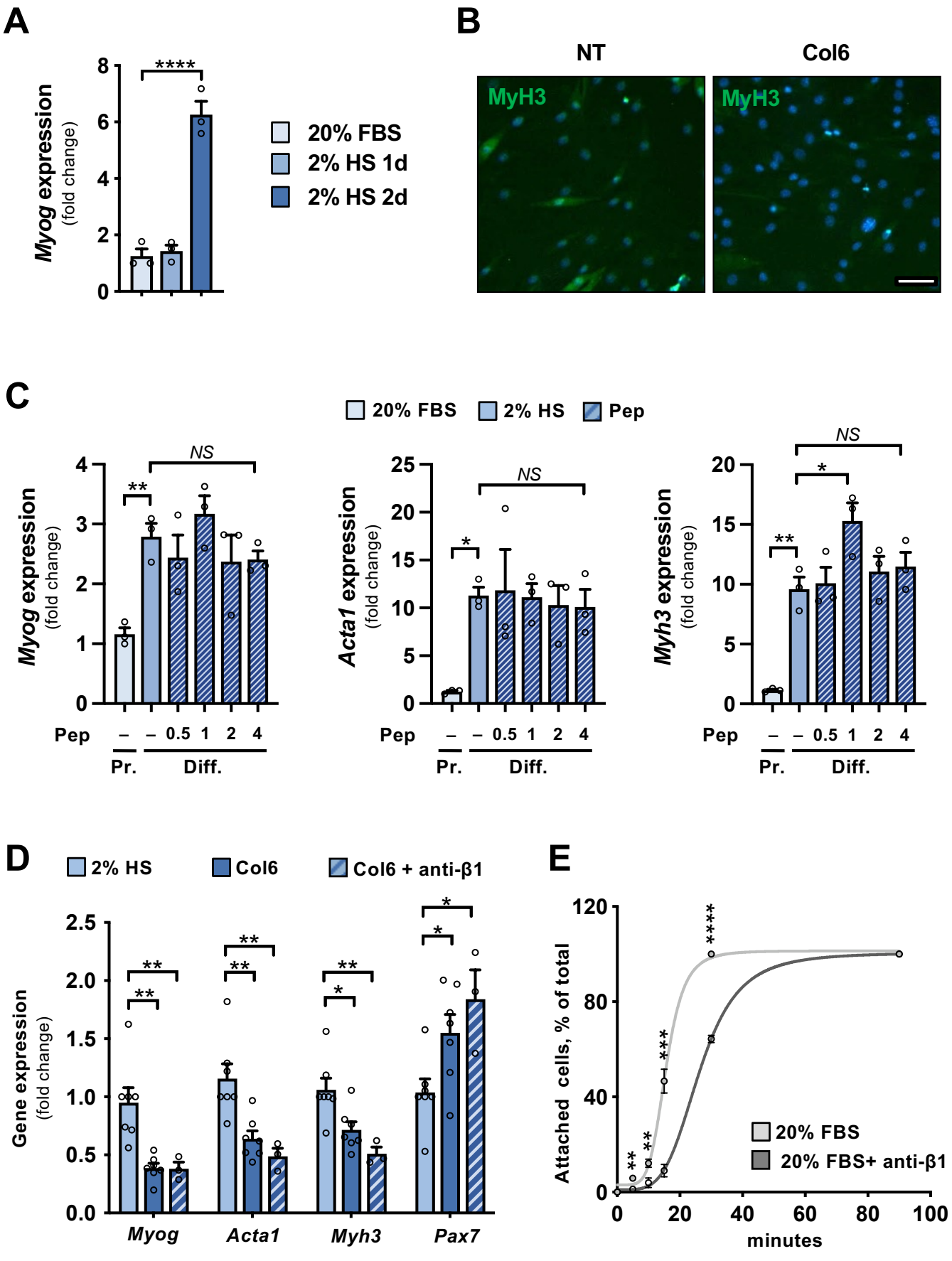
A
Myog expression
(fold change)
****
20% FBS
2% HS 1d
2% HS 2d
B
NT
Col6
MyH3
MyH3
C
20% FBS
2% HS
Pep
Myog expression
(fold change)
Acta1 expression
(fold change)
Myh3 expression
(fold change)
NS
Pep
Pr.
Diff.
D
2% HS
Col6
Col6 + anti-β1
Gene expression
(fold change)
Myog
Acta1
Myh3
Pax7
E
Attached cells, % of total
20% FBS
20% FBS+ anti-β1
minutes

Fig. S1. (**A**) RT-qPCR analysis of *Myog* mRNA levels in proliferating C2C12 cells (20% FBS) and in differentiating C2C12 cells at 1 day (2% HS 1d) and 2 days (2% HS 2d) of differentiation. mRNA levels are shown as fold change compared to the proliferating condition (*n*=3, each condition; ****, *P*<0.0001). (**B**) Representative immunofluorescence for MyH3 (green) in differentiating C2C12 cells maintained for 48 hr in the absence (NT) or presence (Col6) of 4 µg/ml Col6. Nuclei were counterstained with Hoechst (blue). Scale bar, 50 µm. (**C**) RT-qPCR analysis of *Myog, Acta1* and *Myh3* mRNA levels in C2C12 cells maintained for 48 hr in proliferating (Pr.) or differentiating (Diff.) conditions, in the absence of any treatment (–) or treated with different concentrations of pepsin-resistant Col6 fragment (Pep 0.5, 1, 2 and 4 µg/ml). mRNA levels are shown as fold change compared to the proliferating (20% FBS) condition (*n*=3, each condition; *, *P*<0.05; **, *P*<0.01; NS, not significant). (**D**) Gene expression analysis for myogenic differentiation (*Myog*, *Acta1*, *Myh3*) and stemness (*Pax7*) markers, as determined by RT-qPCR of differentiating C2C12 cells maintained for 48 hr in the absence of any treatment (2% HS), or treated with Col6 at 4 µg/ml (Col6), or with 4 µg/ml Col6 in combination with 10 µg/ml β1 integrin inhibitory antibodies (Col6 + anti-β1). mRNA levels are shown as fold change compared to the respective untreated condition (*n*=3-7, each condition; *, *P*<0.05; **, *P*<0.01). (**E**) Percentage of attached C2C12 cells cultured for the indicated time points in proliferating conditions in the absence (20% FBS) or presence (20% FBS + anti-β1) of β1 integrin inhibitory antibodies (*n*=3, each condition; **, *P*<0.01; ***, *P*<0.001; ****, *P*<0.0001).

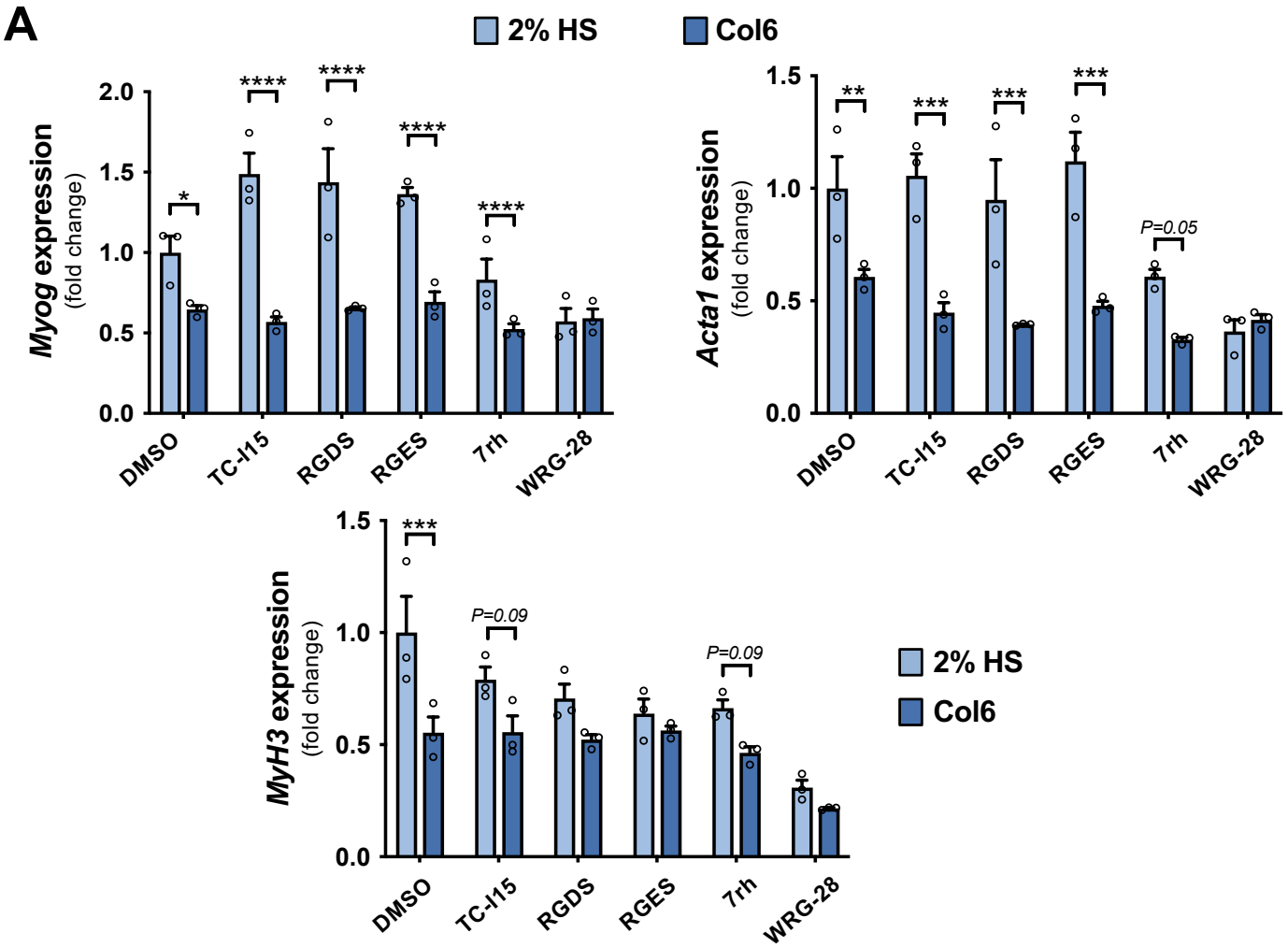

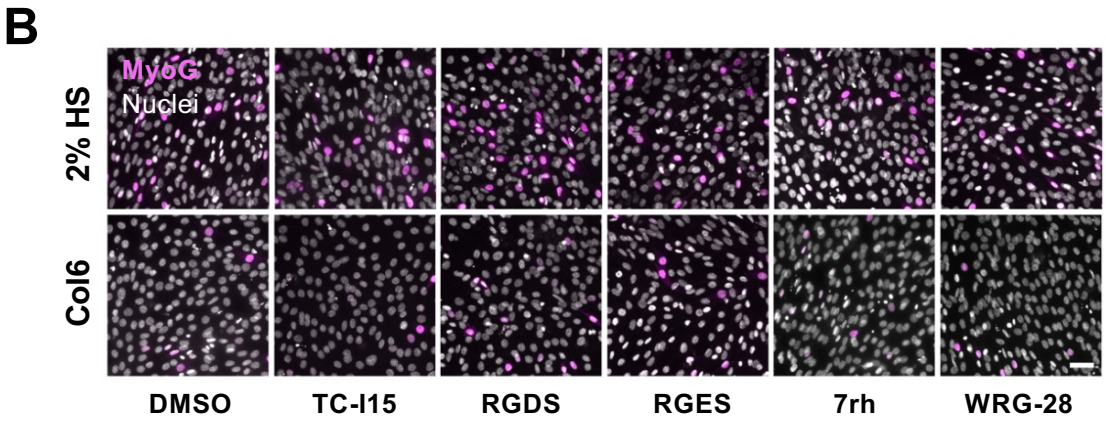

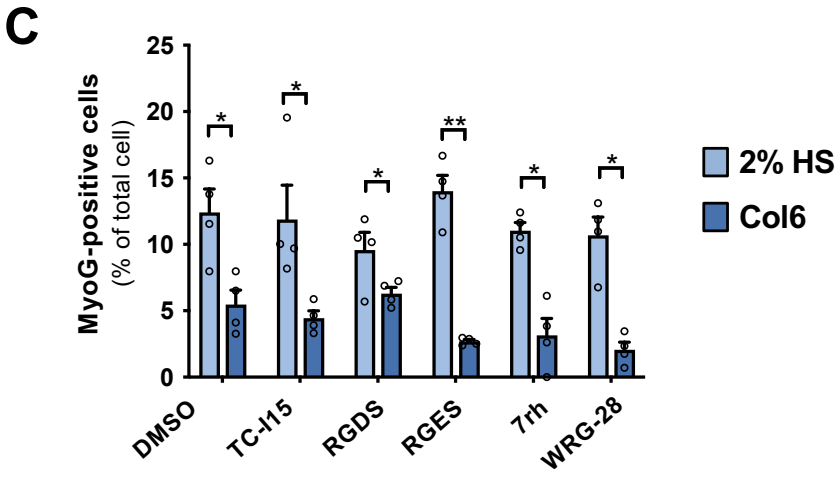

Fig. S2. (A) RT-qPCR analysis of *Myog, Acta1* and *Myh3* mRNA levels in C2C12 cells maintained for 48 hr in differentiating conditions in the absence of any treatment (2% HS) or treated with Col6 at 4 µg/ml (Col6) in combination with the indicated membrane receptor inhibitors (TC-I 15 as an inhibitor of α2β1, α1β1 and α11β1 RGD-independent integrins; RGDS as a broad-spectrum antagonist of RGD-dependent integrins; 7rh and WRG-28 as selective inhibitors of DDR1 and DDR2 collagen receptors, respectively). RGES was as used a negative control for RGDS, whereas DMSO was used as a control for TC-I 15, 7rh and WRG-28. mRNA levels are shown as fold change compared to the DMSO condition (*n*=3, each condition; *, *P*<0.05; **, *P*<0.01; ***, *P*<0.001; ****, *P*<0.0001). (**B**) Representative immunofluorescence for MyoG (magenta) in C2C12 cells maintained for 48 hr in differentiating conditions in the absence of any treatment (2% HS) or treated with Col6 at 4 µg/ml (Col6) in combination with the above membrane receptors inhibitors and their respective controls. Nuclei were counterstained with Hoechst (white). Scale bar, 50 µm. (**C**) Quantification of the percentage of MyoG-positive cells in C2C12 cells maintained for 48 hr in differentiating conditions in the absence of any treatment (2%HS) or treated with Col6 at 4 µg/ml (Col6) in combination with the above membrane receptors inhibitors and their respective controls (*n*=3, each condition; *, *P*<0.05; **, *P*<0.01).

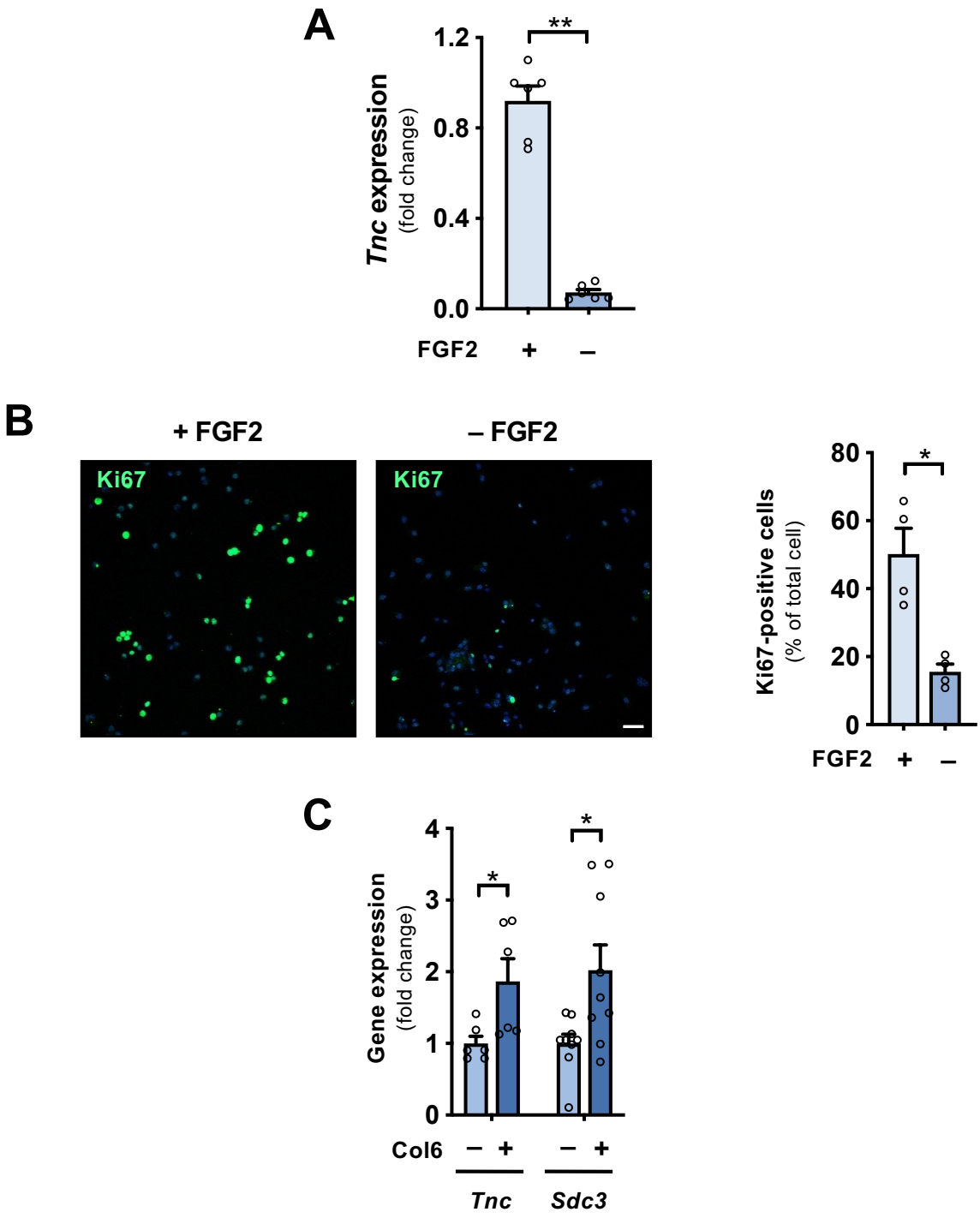

Fig. S3. (**A**) RT-qPCR analysis of *Tnc* mRNA levels in proliferating primary MuSCs (FGF2 +) and in differentiating primary MuSCs maintained for 48 hr in the absence of FGF2 (FGF2 –). mRNA levels are shown as fold change compared to the proliferating condition (n=6, each condition; **, P<0.01). (**B**) Representative immunofluorescence for the proliferation marker Ki67 (green) in primary MuSCs cultured for 48 hr in the presence (+) or absence (–) of 25 ng/ml FGF2. Nuclei were counterstained with Hoechst (blue). Scale bar, 50 µm. Histograms on the right show the quantification of Ki67-positive cells on total cells (n=4, each condition; *, P<0.05). (**C**) RT-qPCR analysis of *Tnc* and *Sdc3* mRNA levels in differentiating primary MuSCs cultured for 48 hr under FGF2 withdrawal in the absence (–) or presence (+) of 4 µg/ml Col6. mRNA levels are shown as fold change compared to the respective untreated condition (n=6-9, each condition; *, P<0.05).

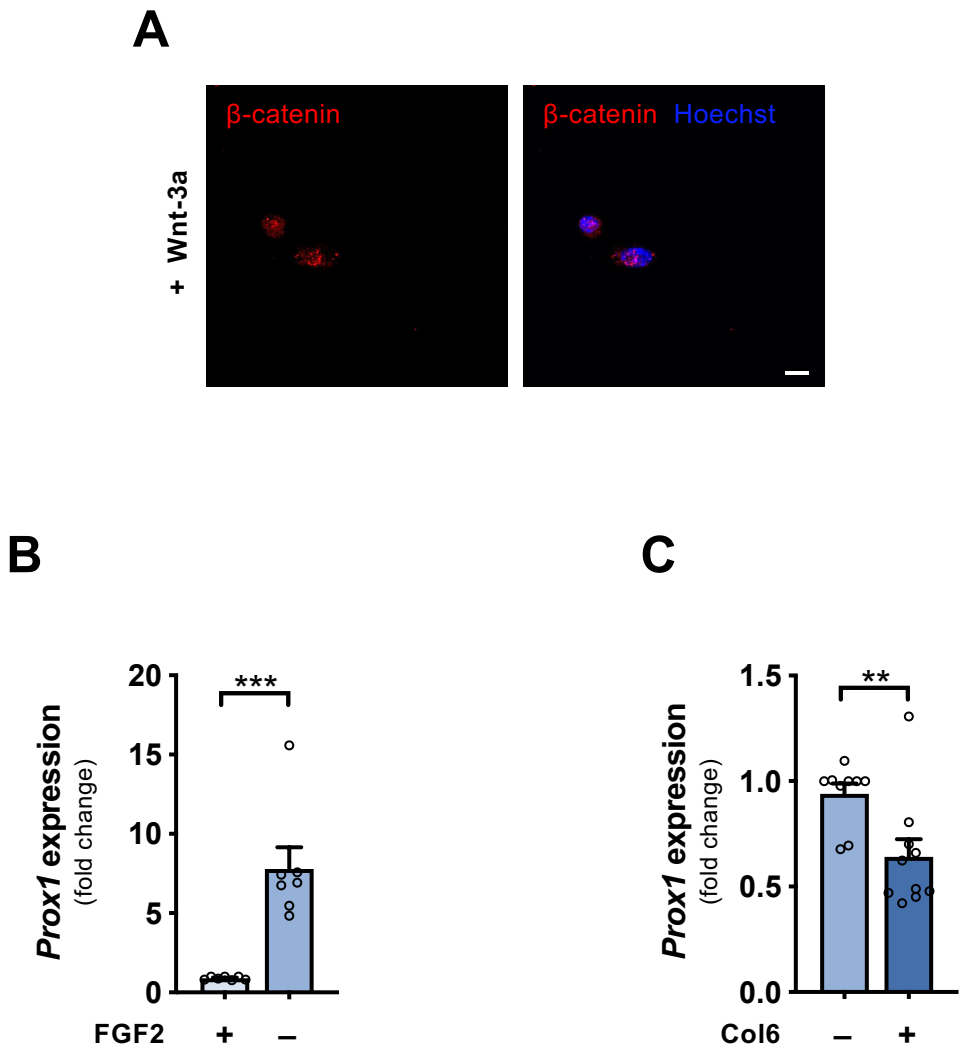

Fig. S4. (**A**) Representative immunofluorescence for β-catenin (red) in primary MuSCs maintained for 48 hr in the absence of FGF2 and treated with 10 ng/ml recombinant Wnt-3a. Nuclei were counterstained with Hoechst (blue). Scale bar, 10 µm.(**B**) RT-qPCR analysis of *Prox1* mRNA levels in proliferating primary MuSCs (FGF2 +) and in differentiating primary MuSCs maintained for 48 hr in the absence of FGF2 (FGF2 –). mRNA levels are shown as fold change compared to the proliferating condition (*n*=6- 7, each condition; ***, *P*<0.001). (**C**) RT-qPCR analysis of *Prox1* mRNA levels in primary MuSCs maintained for 48 hr under FGF2 withdrawal in the absence (–) or presence (+) of 4 µg/ml Col6. mRNA levels are shown as fold change compared to the untreated condition (*n*=9-10, each condition; **, *P*<0.01).

Uncropped gels for Fig. 1B

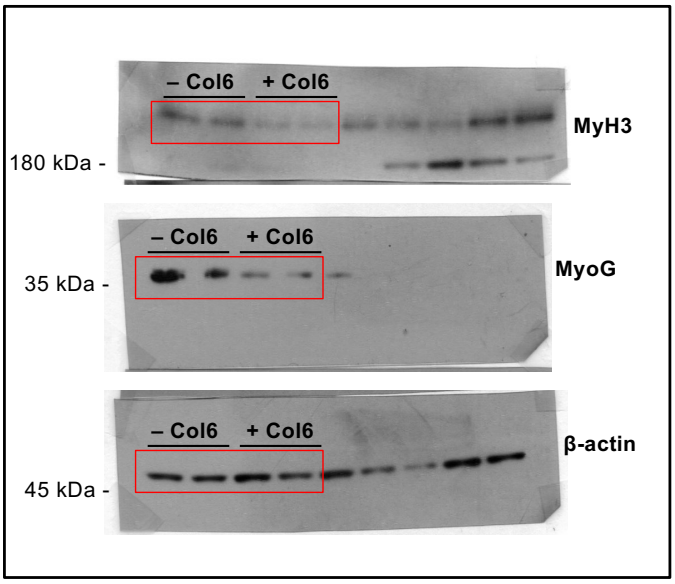

Uncropped gels for Fig. 2C

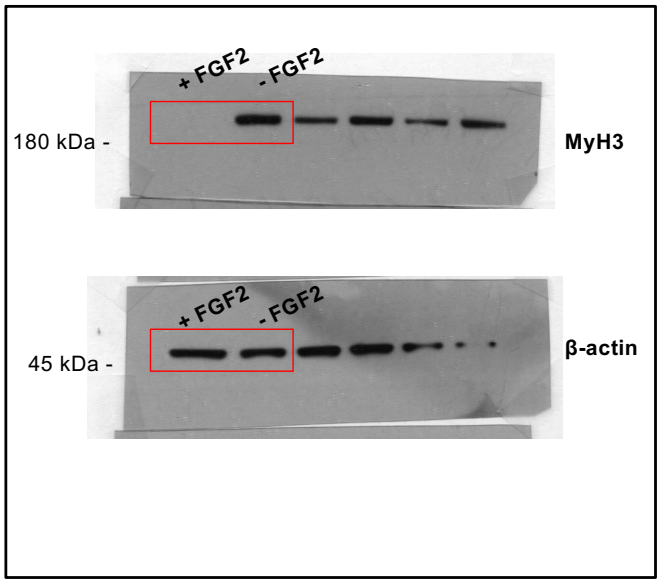

Uncropped gels for Fig. 2D

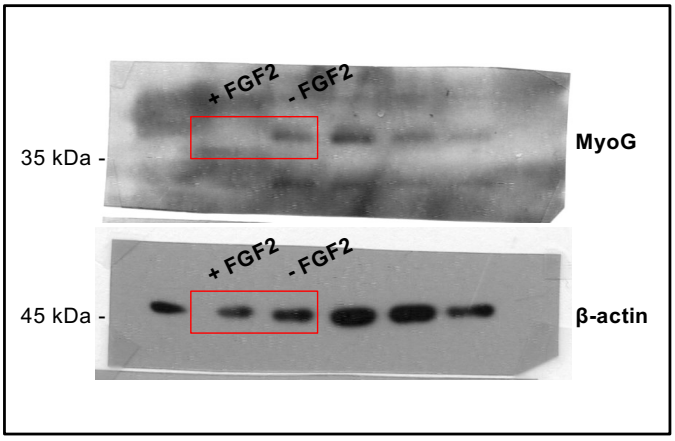

Uncropped gels for Fig. 3F

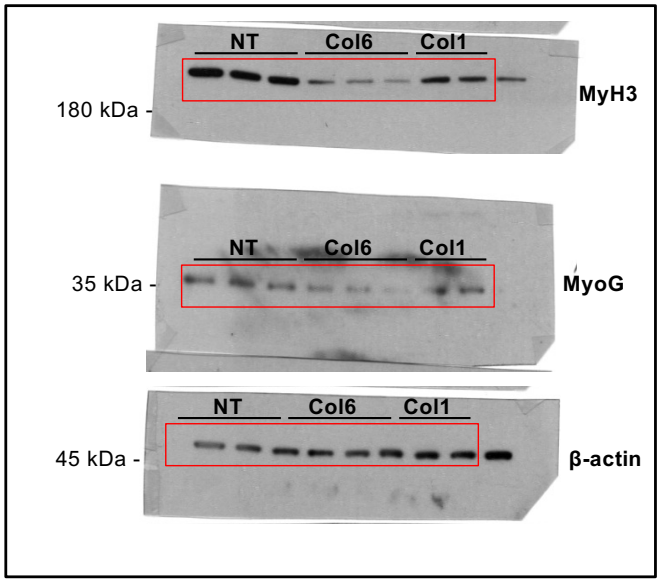

Uncropped gels for Fig. 4B

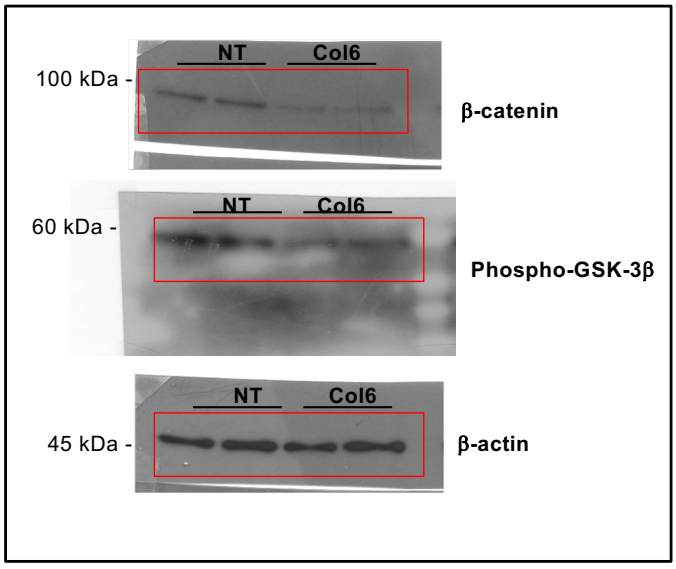

Fig. S5. Blot transparency.

Table S1. List of primers used for RT-PCR experiments.

	Forward (5' > 3')	Reverse (5' > 3')
Acta1	CCCACAACGTGCCCATCTAT	GATGTCGCGCACAATCTCAC
Eya1	CAGCAGACGGGTCTTTAGACA	GGTGAGCTGGTCTTGGACTAAA
Hes1	TGAAGCACCTCCGGAACC	CGCGGTATTTCCCCAACAC
Heyl	GTCCCCACTGCCTTTGAGAA	TCCACGGTCATCTGCAAGAC
Myf5	CCTGTCTGGTCCCGAAAGAAC	GACGTGATCCGATCCACAATG
Myh3	CGCAGAATCGCAAGTCAATA	ATATCTTCTGCCCTGCACCA
Myod	GCTGTCCCTGGTTCTTCACG	TCCTTTCTTTGGGGCTGGAT
Myog	CCCCACTCCCCATTCACATA	CTCCTGAGTTTGCCCCACTG
Notch2	TGGTTCTGGGACAAGTGAACA	ACAGCAAAGCCTCATCCTCA
Notch3	CCATGCCGATGTCAATGCA	TAGCCTCCACGTTGTTCACA
Pax7	CGCTGTGCTGGGACTTCTTC	AGACTCAGGGCTTGGGAAGG
Prox1	GCTACCCCAGCTCCAACATGCT	TGATGGCTTGACGCGCATACTTCT
Tnc	TGGGAAGACGCTAGGGACCG	GAAGAAGGATCTTTTCCAGGTCGG
Sdc3	CTCTGGCTACTTCGAGCAG	CTGGCTGGACTCTTCTACG
S16	GCAGTACAAGTTACTGGAGCC	CGGTAGGATTTCTGGTATCG